

## Design of a One –Dimensional Multilayer Si/SiO<sub>2</sub> Photonic Crystals for Thermophotovoltaic Filters

SAMAH G. BABIKER<sup>1,2</sup>, SHUAI YONG<sup>1\*</sup>, MOHAMED OSMAN SID-AHMED<sup>3</sup> and XIE MING<sup>1</sup>

<sup>1</sup> Department of Engineering Thermophysics-School of Energy Science and Engineering Harbin Institute of Technology, Box. 456, 92 West DaZhi Street, NanGang District, Harbin City, P.R. CHINA Zip Code: 150001

<sup>2</sup> Department of Physics, Faculty of Education, University of the Holy Quran and Islamic Sciences, Omdurman-SUDAN

<sup>3</sup> Department of Physics, Faculty of Sciences, Sudan University of Science and Technology, Khartoum- SUDAN

[samahgas@yahoo.com](mailto:samahgas@yahoo.com) [shuaiyong@hit.edu.cn](mailto:shuaiyong@hit.edu.cn) [mohamedsidahmed5@gmail.com](mailto:mohamedsidahmed5@gmail.com) [xieming@hit.edu.cn](mailto:xieming@hit.edu.cn)

**Abstract:** - In this paper, a one - dimensional multilayer is optimized for potential applications as thermophotovoltaic (TPV) selective filter. The proposed TPV filter was fabricated through a magnetron sputtering process by using the radio frequency (RF) magnetron sputtering system. The spectral reflectance and transmittance of the proposed TPV filter are measured by using spectral transmittance and reflectance measurement system at wavelength from 0.3 $\mu\text{m}$  to 2.5  $\mu\text{m}$  at near normal incident  $8^\circ$ . The bidirectional reflectance/transmittance distribution function BRDF/BTDF are measured by three axis automated scatterometer (TAAS). The calculated spectral reflectance and transmittance of the proposed TPV selective filter has shown several peaks and large oscillations, due to the refractive index mismatch between the proposed TPV filter sample and substrate. The measured results show that the proposed filter has high transmittance value in the spectral range of  $\lambda \leq 1.73\mu\text{m}$  and high  $\text{BTDF} \cdot \cos\theta$  value for both of the TE and TM polarization. It also has low  $\text{BRDF} \cdot \cos\theta$  value at normal incidence due to detector blocks the laser beam. The measured results are in good agreement with the simulation results. The spectral efficiency of the TPV system with the proposed selective filter is above than 0.43 at emitter temperature  $> 1600\text{K}$ . The results show that the 1D 8-layer Si/SiO<sub>2</sub> sample, if used as a selective filter with a low band gap photovoltaic cell (GaSb), would lead to high TPV overall efficiency and high electrical output power. All numerical results are obtained by using the rigorous coupled-wave analysis (RCWA) method.

**Key-Words:** - Thermophotovoltaic, Selective filter, Rigorous coupled wave analysis (RCWA), a magnetron sputtering process, spectral transmittance, bidirectional reflectance/transmittance distribution function.

### 1 Introduction

Thermophotovoltaic (TPV) systems are capable of converting thermal infrared radiation directly into electricity by using photovoltaic effect. They have been considered as energy conversion systems, which allow recycling of the waste heat as well as increasing the conversion efficiency [1-3]. The concept of TPV dates back to 1960s. It was only in recent years that technological improvements in the field of low band gap (0.50 - 0.75) eV photovoltaic cells such as GaSb, GaInAs and GaInAsSb cells and high temperature selective emitting materials, have evoked a renewed interest in TPV generation of electricity [1, 3-4]. The TPV system consists of heat source and optical cavity which comprises of a thermal radiator (emitter), selective filter and photovoltaic PV cell. Advantages TPV system promises to be a very clean and quiet source of electrical power, portable, absence of any moving parts (so low maintenance) and relatively low cost.

As a result, TPV system can be more commonly used in many applications such as remote electrical and thermal energy supplies, transportation, cogeneration of heat and electricity in domestic boilers and it has a very good potential to be an alternative to traditional batteries [1-2, 5-12]. The most obvious drawbacks of TPV systems are their low throughput and poor conversion efficiency, due to a large amount of unusable radiation [1, 13]. The emitter temperature in a TPV system generally ranges between 1000 and 2000 K. This is optimum for a cell with energy gap in the range (0.5 - 0.75) eV [3, 14-16]. Photons having energies higher than the TPV cell bandgap would be absorbed within the depletion region and could produce electricity. Photons having energies less than the TPV cell bandgap (sub-band gap photons) would be absorbed beyond the depletion region due to the long penetration depth of the material at these wavelengths, and cannot produce electricity. These

sub-bandgap photons will result in a destructive heat load on the system components, which will lower the conversion efficiency of the system. In order to reduce the heating and to improve the TPV overall efficiency, these photons should be sent back to the emitter by using filter and back surface reflectors [1, 15]. GaSb, which has low- direct band gap energy of 0.7 eV, is optimum for an emitter temperature of about 1600 K, corresponding to a wavelength of 1.78  $\mu\text{m}$ . This makes it a good choice for a TPV system which transfers the photon energy into electricity. An ideal filter should have high transmittance at short wavelengths and low transmittance at long wavelengths, compared to the bandgap energy [3, 9, 15]. A highly efficient TPV system demands the optimization of the output power and throughput. The conversion efficiency can be improved by controlling the emission spectrum and directions. One possible solution to increase the conversion efficiency and output power is to apply microscale radiation principles in TPV systems. For such purpose, the spectral control of thermal radiation using a selective filter is playing an important role.

One dimensional-photonic crystals (1D PhCs) were used as selective filters in TPV system. They have the advantage of simple structure and that they can easily be fabricated. A cascaded inhomogeneous dielectric substrate with different refractive indexes was tailored as a frequency-selective structure (FSS) and was used as a selective filter for TPV system [17]. 1D photonic crystals which consists of dielectric - dielectric multilayer (Si/SiO<sub>2</sub>) mounted on top of a TPV cell were used in both thermophotovoltaic TPV and micro thermophotovoltaic MTPV systems. They exhibited high efficiency and high power throughput [18]. Samia et al [3] were studied numerically performance of TPV system by using 1D metallic - dielectric photonic crystals (1D MDPCs) which consists of (Ag/SiO<sub>2</sub>). O'Sullivan et al. [19] proposed and fabricated a 10-layers quarter-wave periodic structure (Si/SiO<sub>2</sub>) with the thickness 170 and 390 nm, respectively and suggested reducing the first layer thickness to one half of its original thickness. Mao et al. [9] proposed and fabricated 1D 10-layer by using Si/SiO<sub>2</sub> PhC. More recently, a tandem filter in series with highly doped, epitaxially grown layers was proposed for use as a selective filter in TPV system [20]. The selective filter can be fabrication by using standard photolithographic technique generally. Nghia et al [21] proposed sub-

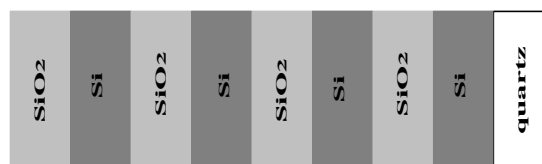
wavelength metallic gratings (the single-layer type and the double-layer) as integrated polarized-RGB color filters and the transmission enhancement was achieved by using a double-layer gratings.

In this paper, the use of 1D 8-layer Si/SiO<sub>2</sub> as selective filter for TPV system having GaSb PV cell is proposed and fabricated.

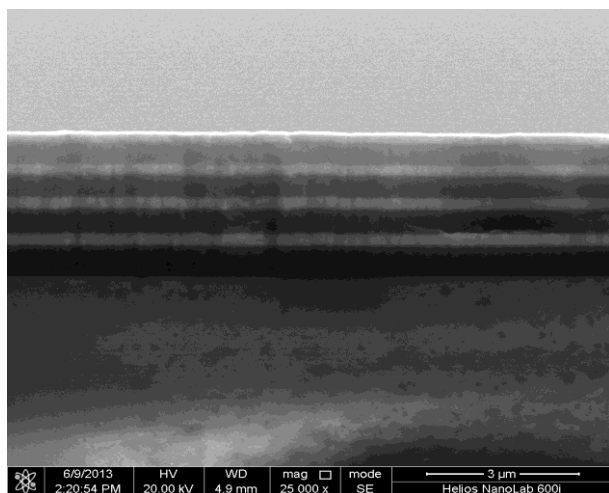
## 2 Numerical Method and Modeling

Rigorous coupled-wave analysis (RCWA), formulated in the 1980s by Moharam and Gaylord, is used for analyzing the diffraction of electromagnetic waves by periodic gratings [22]. It analyzes the diffraction problem by solving Maxwell's equations accurately in each of the three regions (input, multilayer and output), based on Fourier expansion [23]. The diffraction efficiency for each diffraction order is calculated with incident wave properties, feature dimensions, structural profiles and dielectric function of the materials. The dielectric function of the materials is expressed as  $\varepsilon = (n+ik)^2$ , where  $n$  is the refractive index and  $k$  is the extinction coefficient. The accuracy of the solution computed depends solely upon the number of terms retained in space harmonic expansion of electromagnetic fields, which corresponds to the diffraction order. RCWA is used in this study to simulate the radiative properties (spectral reflectance and transmittance) of the periodically, multilayer nanostructures.

Fig.1 is a schematic and scanning electron microscope SEM of the proposed TPV filter considered in this study. The proposed TPV filter consisted of alternating 8-layer (Si/SiO<sub>2</sub>). The thickness of the silicon and silicon dioxide is 160 nm and 440nm respectively, deposited on quartz substrate. The refractive index of Si and SiO<sub>2</sub> are taken to be 3.4 and 1.5 respectively. The electromagnetic wave is incident from air is assumed to be linearly polarized.



(a)



(b)

Fig.1 (a) Schematic of the proposed TPV selective filter (b) SEM image of the proposed TPV selective filter

### 3 Experiment Setup

The proposed TPV filter 1D 8-layer (Si/SiO<sub>2</sub>) is prepared through a magnetron sputtering process. The radio frequency (RF) magnetron sputtering system (JGP450, Shenyang Co. Ltd.) was used to deposit a thin film from sputtering targets onto a substrate and to fabricate multilayer nanostructures filter. The Si and SiO<sub>2</sub> were used as sputtering targets and quartz as the substrate. The sputtering power and pressure were kept at 100 W and 150W for silicon and silicon dioxide, respectively, and operation pressure  $6.7 \times 10^{-4}$  Pa. The base vacuum level was  $6.2 \times 10^{-4}$  Pa. The Ar flow rate was kept at 30 SCCM and controlled by a mass flow meter. A single Si layer was deposited on quartz substrate for 1800 s, and a single SiO<sub>2</sub> layer was deposited on it for 3600s. Fig.2 illustrates the Si and SiO<sub>2</sub> sputtering targets after deposition onto a substrate.

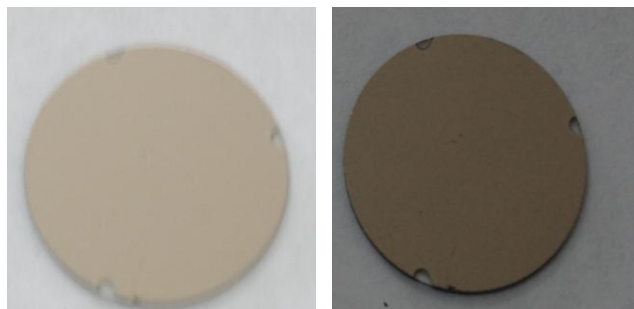


Fig.2 The deposited sputtering targets on a substrate Si (left) and SiO<sub>2</sub> (right)

The thickness of the sputtering targets which were deposited onto a substrate per unit time can be calculated by using the following equations

$$\text{Si: } y = 5.9215x \quad (1)$$

$$\text{SiO}_2: y = 211.7887x \quad (2)$$

Where,  $y$  the thickness of layer per (nm) and  $x$  time of deposition per minute, except eq.2 time per hours.

The deposited rates of the Si and SiO<sub>2</sub> layers are 0.0987 nm/s and 0.0588 nm/s, respectively. Scanning electron microscope SEM was used for characterization of the surface topography and morphology of the selective TPV filter. The sample, before SEM, was coated by a thin layer of conductive material (gold), as shown in Fig.3. The spectral transmittance and reflectance measurement system was employed to measure the spectral reflectance and transmittance at wavelength  $\lambda$  from 0.3 μm to 2.5 μm. The bidirectional reflectance/transmittance distribution function BRDF/BTDF is defined as the ratio of the reflected/transmitted power to the incident power [24]. Three-axis automated scatterometer TAAS was used to measure BRDF/ BTDF of the TPV filter sample at normal incident and  $\lambda = 660\text{nm}$  for both of the TE and TM polarization. It was also used to measure the BRDF at different incidence angles for TM polarization. The measured results for the spectral reflectance and transmittance were compared with the simulation results those obtained by RCWA method.

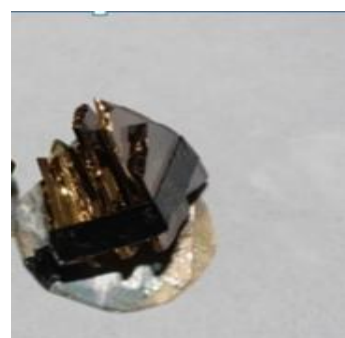


Fig.3 The image of the proposed selective TPV filter sample before SEM

## 4 Results and Discussion

### 4.1 Spectral reflectance measurements for the proposed TPV filter

The spectral reflectance of the proposed TPV filter is measured by using spectral transmittance and reflectance measurement system at wavelength  $\lambda$

from 0.3  $\mu\text{m}$  to 2.5  $\mu\text{m}$  and near normal incident  $8^\circ$ . The results were compared with the simulation results. It can be noted from Fig.4 that the highest spectral reflectance value for the proposed TPV filter exceeds 0.7 and 0.4 at  $\lambda \leq 1.73\mu\text{m}$  in both of the simulation results and experimental results, respectively. Furthermore, it has several peaks and large oscillations in the spectral reflectance when it was calculated numerically at  $\lambda \leq 1.73\mu\text{m}$ . These are caused by the refractive index mismatch between the proposed TPV filter and the substrate. It also reflects most of the radiated photons in wavelength from 1.73 to 3.9  $\mu\text{m}$ . In order to reduce the spectral reflectance oscillations of the selective filter and improve the performance we propose to reduce the thickness of the first layer of  $\text{SiO}_2$  to half of its original thickness to form anti-reflection coating.

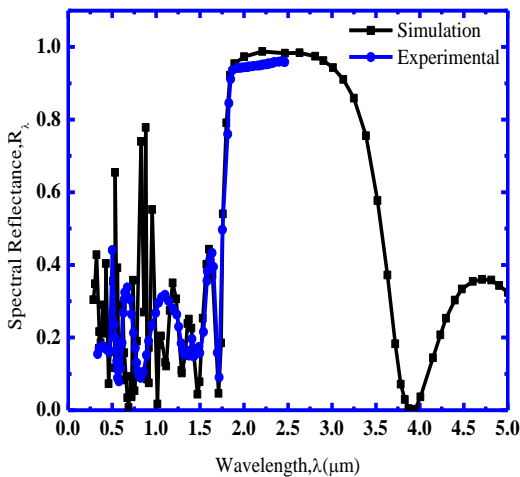


Fig.4 Measured and simulation spectral reflectance of the proposed TPV selective filter at  $\theta = 8^\circ$

#### 4.2 Spectral transmittance measurements for the proposed TPV filter

The spectral transmittance of the proposed TPV filter also is measured at  $\theta = 8^\circ$  by using spectral transmittance and reflectance measurement system. The results are compared with the simulation results as shown in Fig.5. We note that the values calculated numerically exhibits several peaks and larger oscillations compared to experimental results. The results show the spectral transmittance for the proposed TPV filter about 0.95 at  $\lambda = 1.73\mu\text{m}$ . The emitter temperature in a TPV system generally ranges between 1000 and 2000 K; that means the fraction of the power above the electronic band-gap ( $E_g$ ) in the total radiated power is quite small even

for GaSb cells with a band-gap of 0.7 eV, which would lead to extremely poor overall system efficiency and power density. So, the enhancement of TPV efficiency can be achieved by using selective filter which reflects below band-gap photons back to the emitter for re-radiation and transmits above band-gap photons to the cells.

Based on both of the simulation and experimental results, proposed TPV filter can serve as selective filter in TPV applications. The Si and  $\text{SiO}_2$  materials have low absorption coefficients in the near-infrared region, so they can be used for fabrication of a wavelength selective filter. The experimental results are in good agreement with the simulation results.

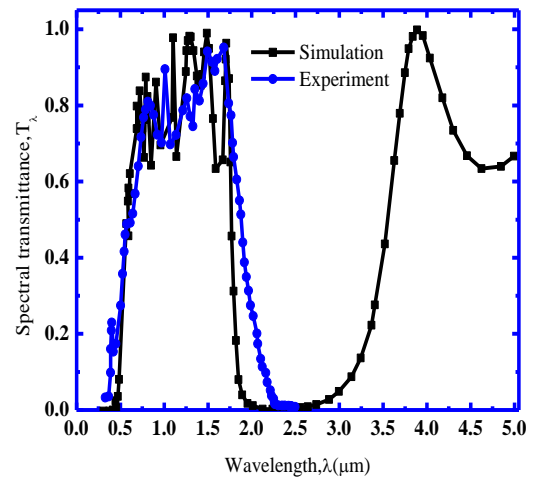


Fig.5 Measured and simulation spectral transmittance of the selective filter at  $\theta = 8^\circ$

#### 4.3 BRDF measurements for the proposed TPV filter

##### 4.3.1 Effect of the polarization on BRDF of the proposed TPV filter

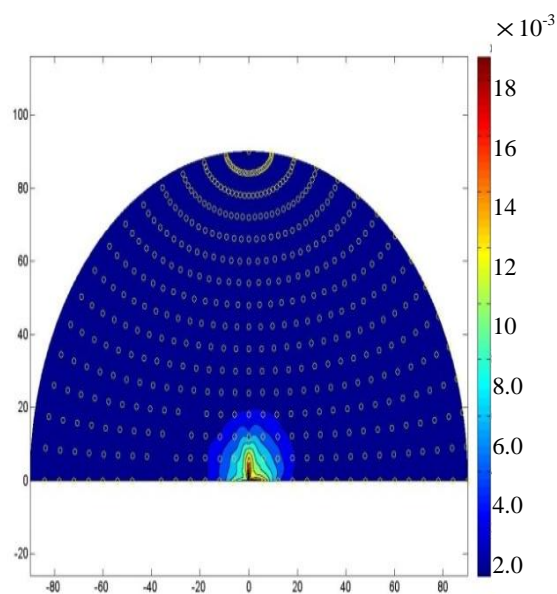
The reflectance distribution  $\text{BRDF} \cdot \cos\theta$  in the half hemispherical space over the TPV filter surface at normal incident,  $\lambda = 660\text{nm}$ , is measured by using TAAS instrument for TE and TM polarization, respectively. The results are plotted in polar coordinates system (where the radial axis denotes zenith angle  $\theta$  and the polar angle denotes the azimuthal angle  $\phi$ ) as shown in Fig. 6. The incident laser beam was focused on the sample at spot, which corresponds to the collimator diameter of about 5mm and the blue color in the figure denotes the reflectance places. The results show that the TPV filter has the same maximum value of  $\text{BRDF} \cdot \cos\theta$  about 1.8% for both of TE and TM



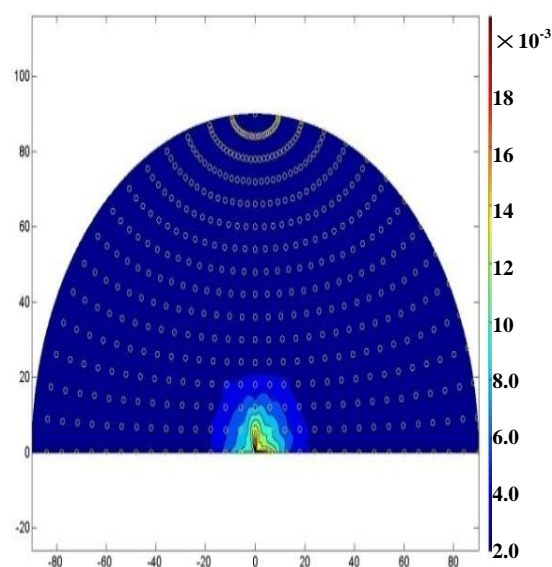
polarization. The measured values of  $\text{BRDF} \bullet \cos\theta$  are very low and the accuracy is not expected to be high. When the detector was positioned in front of the laser beam path, it blocks the laser beam and reflectance could not be obtained, because of the shadowing effect. The invalid data has been removed from the data set during post processing of the BRDF data. The TPV filter sample has a low  $\text{BRDF} \bullet \cos\theta$  value means high transmitted energy and that most of the incident energy has passed through the sample. This is required for optimum performance of an ideal selective filter in thermophotovoltaic applications.

#### 4.3.2. Effect of the plane of incidence on BRDF of the proposed TPV filter

Fig.7 shows effect of the plane of incidence (PoI) on the BRDF of the filter in the half hemispherical space at different angles ( $0^\circ, 15^\circ, 30^\circ, 45^\circ, 60^\circ$  and  $75^\circ$ ) at wavelength  $\lambda = 660\text{nm}$  for TM wave. As can be seen from the figures, a strange reflecting characteristic of the TPV filter sample can be observed, namely, the maximum measured value of  $\text{BRDF} \bullet \cos\theta$  has lower value at  $\theta = 0^\circ$ , while higher value at  $\theta = 30^\circ$ . It has the same value, about 4%, when the laser beam incident on the TPV filter sample at  $\theta = 45^\circ$  and  $\theta = 60^\circ$  and also we can note two values of  $\text{BRDF} \bullet \cos\theta$  at the forward and the backward direction. The maximum measured value of the reflectance distribution at the forward direction is greater than the backward at these angles. As seen from the figures, the proposed TPV filter has low reflectance energy and most of the energy can be passed through the sample. The results explain the plane of incidence influence on the  $\text{BRDF} \bullet \cos\theta$  of the proposed TPV filter. Fig.8 shows the reflectance distribution in the incident plane at different incident angles all with  $\varphi_i = 0^\circ$ . It can be noted that, at zenith angle  $\theta_r = 30^\circ$  the reflectance distribution  $\text{BRDF} \bullet \cos\theta$  has higher values, more than 40%, at azimuthal angle  $\varphi_i = 0^\circ$  compared to other angles, while it has lower value at  $\theta_r = 0^\circ$ . So, based on the measured results of BRDF, the sample is suitable to be used as a selective filter in all TPV applications to improve TPV overall efficiency and enhances the electrical output power.

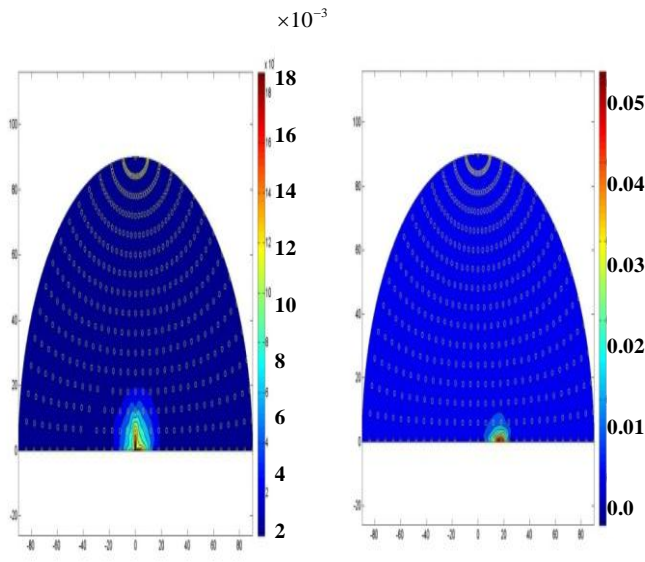


(a)



(b)

Fig.6 The  $\text{BRDF} \bullet \cos\theta$  of the proposed TPV filter at normal incident for (a) TE wave (b) TM wave



$\theta = 0^\circ, \varphi_i = 0^\circ$

$\theta = 15^\circ, \varphi_i = 0^\circ$

$\theta = 60^\circ, \varphi_i = 0^\circ$        $\theta = 75^\circ, \varphi_i = 0^\circ$

Fig.7 The  $BRDF \bullet \cos\theta$  of the proposed TPV filter at different incident angles in the polar coordinates for TM wave

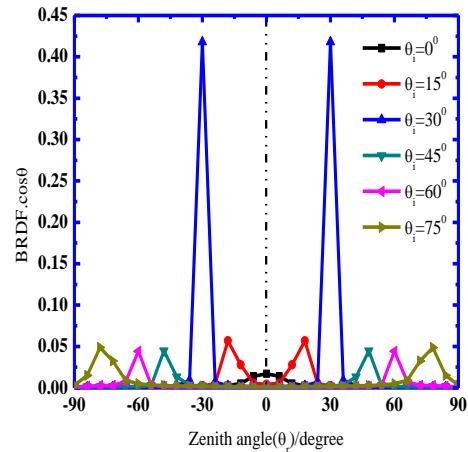
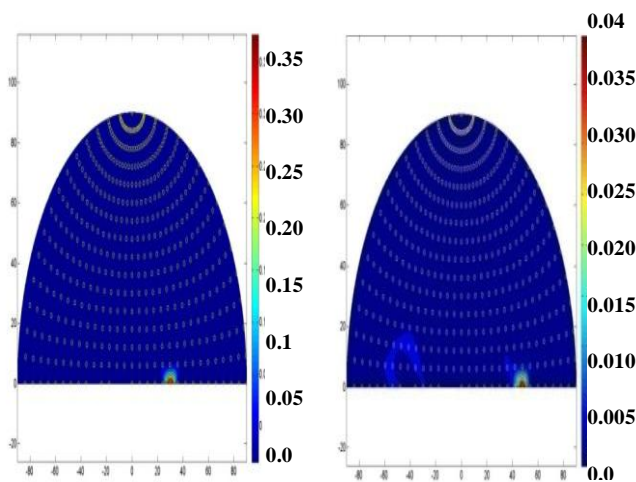
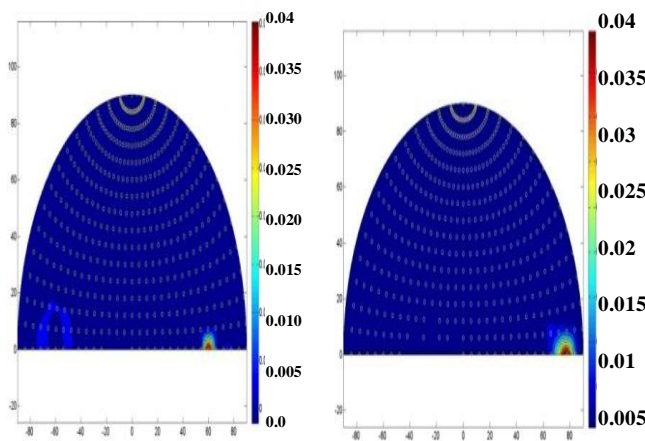


Fig.8 The  $BRDF \bullet \cos\theta$  of the proposed TPV filter incident plane at different incident angles all with  $\varphi_i = 0^\circ$



$\theta = 30^\circ, \varphi_i = 0^\circ$

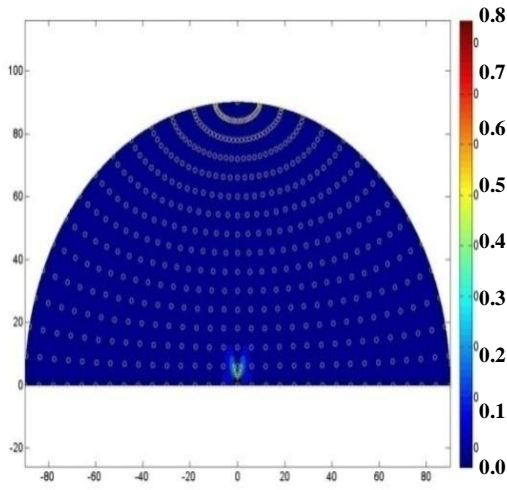
$\theta = 45^\circ, \varphi_i = 0^\circ$



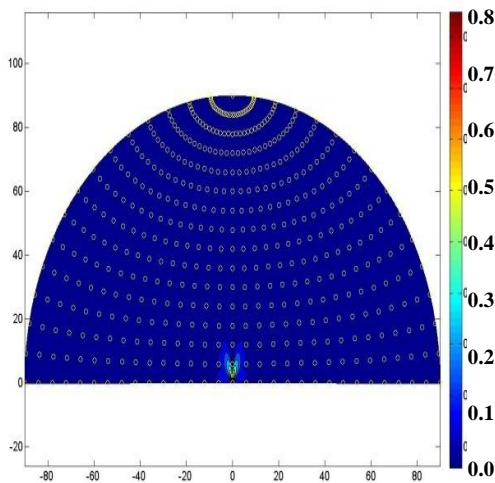
#### 4.4 BTDF measurements for the proposed TPV filter

Fig.9 shows the measured results of  $BTDF \bullet \cos\theta$  in the half hemispherical space over the TPV filter surface at normal incident,  $\lambda = 660\text{nm}$  for TE and TM polarization, respectively. As seen from the results, there is no difference in the transmittance distribution for both of TE and TM polarization. The sample has the same maximum value of the  $BTDF \bullet \cos\theta$  about  $80\% < BTDF \bullet \cos\theta < 90\%$  for both of TE and TM polarization. The maximum value of  $BTDF \bullet \cos\theta$  for TPV selective filter is expected to be higher than the measured value. When the laser beam is incident on the sample at  $\theta = 0^\circ$  most of the energy is transmitted through the TPV selective filter and little part of the energy is reflected and scattered outside TPV selective filter surface. The part of the energy which is reflected from the TPV selective filter has been discussed in the above section of BRDF. 1D 8-layer Si/SiO<sub>2</sub> sample has the characteristics of an ideal selective filter with high transmittance at short wavelengths and low reflectance at long

wavelengths, compared to the band gap energy. So, it can be used as a selective filter with a GaSb, low band gap cell, in TPV applications.



(a)



(b)

Fig.9 The  $BTDF \cdot \cos\theta$  of 1D 8-layer Si/SiO<sub>2</sub> sample at normal incident for (a) TE (b) TM wave

### 5 TPV System Performance

The efficiency of the proposed selective filter is characterized by the spectral efficiency  $\eta_{sp}$  which is defined as [19],

$$\eta_{sp} = \frac{P_A}{P_{net}} \tag{3}$$

$$P_A = \frac{2\pi}{c^2 h^3} \int_{E_g}^{\infty} \frac{E^3}{\exp(E/kT_{emt}) - 1} \bar{T}_f(E) dE \tag{4}$$

$$P_{net} = \frac{2\pi}{c^2 h^3} \int_0^{\infty} \frac{E^3}{\exp(E/kT_{emt}) - 1} \left(1 - \bar{R}_f\right)(E) dE \tag{5}$$

Where,  $P_A$  is the above-bandgap power transmitted through the filter to the PV cell,  $P_{net}$  is the net power to the filter from emitter,  $h$  is Planck's constant,  $c$  is the speed of light,  $E$  is the photon energy,  $k$  is Boltzmann's constant,  $T_{emt}$  is the emitter temperature and  $E_g$  is the electronic band-gap of the cell. From the above equations the spectral efficiency of the proposed filter can be expressed as

$$\eta_{sp} = \frac{\int_{E_g}^{\infty} \frac{2\pi E^3}{c^2 h^3} \frac{1}{\exp(E/kT_{emt}) - 1} \bar{T}_f(E) dE}{\int_0^{\infty} \frac{2\pi E^3}{c^2 h^3} \frac{1}{\exp(E/kT_{emt}) - 1} \left(1 - \bar{R}_f(E)\right) dE} \tag{6}$$

Where  $\bar{T}_f$  and  $\bar{R}_f$  are defined as the average spectral transmittance and reflectance of the filter, respectively.

An ideal filter would yield a unity spectral efficiency by transmitting all the photons of energy above  $E_g$  to the cell ( $\bar{T}_f(E) = 1$  for  $E \geq E_g$ ) and reflecting all the other photons back to the radiator ( $\bar{R}_f(E) = 1$  for  $E < E_g$ ). The spectral efficiency of

TPV system with the proposed filter as a function of the emitter temperature was calculated with the proposed 1D PhC filter. Fig.10 shows the dependence of the spectral efficiency on the emitter temperature. It can be seen that the spectral efficiency increases when the emitter temperature increases and it is above than 0.43 at  $T_{emt} > 1600K$ .

The simulation results are in good agreement with the results of Ref [9]. GaSb, which has low- direct band gap energy of 0.7 eV, is optimum for an emitter temperature of about 1600 K, corresponding to a wavelength of 1.78  $\mu m$  [3] is good photovoltaic cell to use as TPV cell with the 1D 8-layer Si/SiO<sub>2</sub> as a selective filter, to improve of TPV efficiency and enhancement of electrical output power.



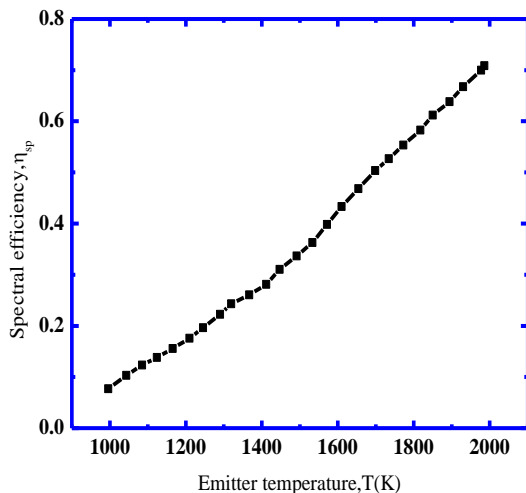


Fig.10 Spectral efficiency of the TPV systems as function of the emitter temperature with the proposed 1D multilayer (Si/SiO<sub>2</sub>) selective filter for TM wave

## 6 Conclusion

In order to enhance TPV overall efficiency and electrical output power, we proposed 1D 8-layer nanostructure TPV selective filter. The spectral reflectance, transmittance and bidirectional reflectance/transmittance distribution function BRDF/BTDF of the proposed TPV filter are experimentally measured. The maximum measured transmittance value of the proposed filter is about 95% at wavelength 1.73  $\mu\text{m}$ . It also reflects most of the radiated photons in wavelength from 1.73 to 3.9  $\mu\text{m}$ . Several peaks and large oscillations in the spectral transmittance and reflectance when it was calculated numerically at  $\lambda \leq 1.73 \mu\text{m}$ . These are caused by the refractive index mismatch between the proposed TPV filter and the substrate. The measured results show that the proposed filter has high reflectance distribution value  $\text{BRDF} \cdot \cos\theta$  at zenith angle  $\theta_r = 30^\circ$ , while it has low value at  $\theta_r = 0^\circ$ . The measured results are in good agreement with the simulation results. The spectral efficiency of the TPV system with the proposed selective filter is about 0.43 at emitter temperature 1600 K. The performance of the proposed TPV filter recommends it to be used in TPV applications, with GaSb cell (low band gap cell), as an efficient power generator.

## Acknowledgements

This work is supported by the Foundation for Innovative Research Groups of the National Natural Science Foundation of China (No. 51276049) and the Fundamental Research Funds for the Central

Universities (No. HIT. BRETIII.201227). A very special acknowledgement is made to the editors and referees whose constructive criticism has improved this paper.

## References:

- [1] S. Basu, Y.-B. Chen, & Z. M. Zhan, Microscale radiation in thermophotovoltaic devices - A review, *International Journal of Energy Research*, Vol.31, 2007, pp.689-716.
- [2] L. P. Wang, & Z. M. Zhang, Wavelength-selective and diffuse emitter enhanced by magnetic polaritons for thermophotovoltaics, *Applied Physics Letters*, Vol. 100,2012,p.063902(3pages).
- [3] S. I. Mostafa, N.H.Rafat, & S.A. El-Naggar, One-dimensional metallic-dielectric (Ag/SiO<sub>2</sub>) photonic crystals filter for thermophotovoltaic applications, *Renewable Energy*, Vol.45,2012,pp.245-250.
- [4] E. Nefzaoui, J. Drevillon, &K. Joulain, Selective emitters design and optimization for thermophotovoltaic Applications, *Applied Physics*, Vol. 111,2012,pp.084316.
- [5] T.J. Coutts, A review of progress in thermophotovoltaic generation of electricity, *Renewable and Sustainable Energy Reviews*, Vol.3 (2), 1999, pp.177-184.
- [6] T.J. Coutts, An overview of thermophotovoltaic generation of electricity, *Solar Energy Materials & Solar Cells*, Vol. 66,2001,pp.443-452.
- [7] K. Qiu, & S.C.A. Hayden, Development of a silicon concentrator solar cell based TPV power system, *Energy Conversion and Management*, Vol. 47,2006,pp.365-376.
- [8] N. Z. Jovanovic, Two-Dimension Photonic Crystals as Selective Emitters for Thermophotovoltaic Power Conversion Applications (Thesis), Massachusetts Institute of Technology, Jun,2005.
- [9] L. Mao, &H. Ye, New Development of One-Dimensional Si/SiO<sub>2</sub> Photonic Crystals Filter for Thermophotovoltaic Applications, *J. Renewable Energy*, Vol.35, 2010,pp. 249-256.
- [10] M.W. Yang, K.S. Chou, C. Shu, W. Z. Li, & H. Xue, Research on micro-thermophotovoltaic power generators, *Solar Energy Materials & Solar Cells*, Vol.80, 2003, pp. 95-104.
- [11] X. Wu, H. Ye, & J. Wang, Experimental analysis of cell output performance for a TPV



- system, *Solar Energy Materials & Solar Cells*, 2011, 95:2459-2465.
- [12] X. Yimin, C. Xue, & H. Yuge, Design and analysis of solar thermophotovoltaic systems, *Renewable Energy*, Vol. 36, 2011, pp.374-387.
- [13] T.J. Coutts, G. Guazzoni, & J. Luther, Thermophotovoltaic Generation of Electricity: *Fifth Conference on Thermophotovoltaic Generation of Electricity*, Rome, Italy, 2003, 16-19 September 2002.
- [14] N.N. Lal & W.A. Blakers, Silver cells in thermophotovoltaic systems, *Solar Energy Materials & Solar Cells*, Vol.93, 2009, pp.167-175.
- [15] L. C. Chia, & B. Feng, The development of a micropower (micro-thermophotovoltaic) device (Review), *Power Sources*, Vol. 165, 2007, pp. 455-480.
- [16] V. Badescu, Thermodynamic theory of thermophotovoltaic solar energy conversion. *Applied Physics*, Vol. 90(12), 2001, pp. 6476-6486.
- [17] G. Kiziltas, L.J. Volakis, & N. Kikuchi, Design of a frequency selective structure with inhomogeneous substrates as a thermophotovoltaic filter, *IEEE Transactions on Antennas and Propagation*, Vol. 53 (7), 2005, pp.2282-2289.
- [18] I. Celanovic, F. O'Sullivan, M. Ilak, J. Kassakian, & D. Perreault, Design and optimization of one-dimensional photonic crystals for thermophotovoltaic applications, *Optics Letters*, Vol. 29 (8), 2004, pp.863-865.
- [19] F. O'Sullivan, I. Celanovic, N. Jovanovic, J. Kassakian, S. Akiyama, & K. Wada, Optical characteristics of one dimensional Si/SiO<sub>2</sub> photonic crystals for thermophotovoltaic applications, *Journal of Applied Physics*, Vol.97 (3), 2005, pp.033529.
- [20] P.M. Fourspring, D.M. DePoy, T.D. Rahmlow, J.E. Lazo-Wasem, & E.J. Gratrix, Optical coatings for thermophotovoltaic spectral control, *Applied Optics*, Vol. 45(7), 2006, pp.1356-1358.
- [21] N. Nguyen-Huu, Y.-L. Lo, Y.-B. Chen & T.-Yu. Yang, Subwavelength Metallic Gratings as an Integrated Device: Polarized Color Filter, *Proc. of SPIE*, Vol. 7934, 2011, pp.79340U (1-10).
- [22] S. Peng, & G. M. Morris, Efficient implementation of rigorous coupled-wave analysis for surface-relief gratings, *Opt. Express*, Vol. 12(5), 1995, pp.1087-1096.
- [23] M. G. Moharam, & T. K. Gaylord, Rigorous coupled-wave analysis of planar-grating diffraction, *Opt. Express*, Vol. 71(7), 1981, pp. 811-818.
- [24] J.Y. Shen, Z.Q. Zhu, & M.Z. Zhang, A Scatterometer for Measuring the Bidirectional Reflectance and Transmittance of Semiconductor Wafers with Rough Surfaces, *Review of Scientific Instruments*, Vol.74, 2003, pp. 4885-4892.